Electronic Supplementary Information

Single-Step Bioassays in Serum and Whole Blood with a Smartphone, Quantum Dots and Paper-in-PDMS Chips

Eleonora Petryayeva and W. Russ Algar*

Department of Chemistry, University of British Columbia, 2036 Main Mall, Vancouver, British Columbia, V6T 1Z1, Canada

*To whom correspondence should be addressed. E-mail: algar@chem.ubc.ca

Table of Contents

1. Detailed Experimental Methods

1.1 Materials and Reagents

Lipoic acid (LA, ≥99%), *N,N'*-diisopropylcarbodiimide (DIC, >98%), *N*,*N*-diisopropyl-ethylamine (DIPEA, ≥99%) *N*-hydroxysuccinimide (NHS, 98%), succinic anhydride, ethylenediamine, tetramethylammonium hydroxide (TMAH) solution in methanol (25% w/v), sodium borohydride (≥98%), sodium cyanoborohydride (95%), sodium (meta)periodate (≥99%), glutathione (GSH), streptavidin (SAv), and bovine serum (adult) were from Sigma-Aldrich (Oakville, ON, Canada). EZ-Link amine-PEG_3-biotin (biotinyl-3,6,9,-trioxaundecanediamine), ammonium acetate, sodium hydroxide, acetic acid, and boric acid were from Fisher Scientific (Ottawa, ON, Canada). A polydimethylsiloxane (PDMS, Sylgard 184) elastomer kit was obtained from Dow Corning (Midland, MI, USA). Defibrinated bovine blood was from Hemostat Laboratories (Dixon, CA, USA). Human alpha-thrombin was from Haematologic Technologies (Essex Junction, VT, USA).

Peptides were from Bio-Synthesis Inc. (Lewisville, TX, USA) and their sequences are listed in Table S1. Alexa Fluor 647 (A647) C2 maleimide dye, Alexa Fluor 680 (A680) C2 maleimide dye, and streptavidin Alexa Fluor 647 (SAv-A647) conjugate were purchased from Life Technologies (Carlsbad, CA, USA). Buffers were prepared with water purified by a Barnstead Nanopure water purification system (Thermo Scientific, Ottawa, ON, Canada) and sterilized by autoclaving prior to use. Buffers included borate buffer (50 mM, pH 9.2 and 50 mM, pH 8.5), and phosphate buffered saline (PBS; 12 mM phosphate, 137 mM NaCl, 2.7 mM KCl, pH 7.4).

Table S1. Peptide substrate sequences.

Amino acid sequence (written N-terminal to C-terminal) [a,b,c]	Abbreviation	Assay [d]
(1) Ace-HHHHHHSPPPPPPGSDGNESG**LVPR**↓GSGC(A647)	Sub(A647)	THR (sample spot)
(2) Ace-HHHHHHSPPPPSGNLGNDSGWDSGNDSGN	Pep	THR and SAv (reference spot)
(3) Biotin-PEG_3-GSGP_4GSGHHHHHH-Am	Pep(Biotin)	SAv (sample spot)

[a] The protease recognition site is indicated in bold and the hydrolysis position is indicated by the downwards arrow; [b] Ace = acetylated; [c] PEG_3 = –NH–[CH_2–CH_2–O]$_3$–CH_2–CH_2–NH–; Am = amidated; [d] THR = thrombin, SAv = streptavidin.

1.2 QD Ligand Exchange with Glutathione

Organic TOPO/HDA capped QDs dispersed in toluene were washed once with absolute ethanol by precipitation (4800 rcf, 4 min). The supernatant was discarded and the pellet redissolved in toluene. GSH-QDs were prepared by diluting 100 μL (10–20 μM in toluene) of organic QDs to 1 mL with $CHCl_3$ and adding a solution of GSH (100 mg) prepared in 300 μL of TMAH (25% w/v) in methanol. This mixture was vortexed and allowed to stand overnight. GSH-coated QDs were subsequently extracted into 200 μL of borate buffer (pH 9.2, 50 mM, 250 mM NaCl) and the organic layer discarded. The GSH-coated QDs were precipitated with ethanol (*ca.* 1 mL) by centrifugation (4800 rcf, 4 min), redispersed in 200 μL of buffer, and then washed twice more with ethanol. After the final wash, QDs were dissolved in borate buffer (pH 9.2, 50 mM) and stored at 4 °C.

1.3 Peptide Modifications

1.3.1 Dye-Labeled Peptides

Peptide **1** (see Table S1) with a terminal cysteine residue was labeled with Alexa Fluor 647 C2 maleimide dye (or Alexa Fluor 680 C2 maleimide) according to previously published protocols with slight modifications.[1] Briefly, 1.0 mg (0.33 μmol) of peptide was dissolved in 50 μL of 50% v/v MeCN:water, diluted with 350 μL of PBS and mixed with ~0.5 mg (0.4–0.5 μmol) of A647 (or A680) dye dissolved in 25 μL of DMSO. The reaction was placed on a mixer for 24 h at room temperature in the dark. Labeled peptide was separated from excess dye using nickel(II) nitrilotriacetic acid (Ni-NTA) agarose and subsequently desalted using Amberchrom CG300M chromatographic grade resin (Dow Chemical, Midland, MI, USA). Peptides were quantitated using UV-visible spectrophotometry. The peptide was aliquoted into 20 nmol fractions, dried under vacuum, and stored at –20 °C until needed.

1.3.2 Biotinylated Peptide

The *N*-terminus of peptide **3** (see Table S1) was first reacted with succinic anhydride to convert it to carboxylic acid. Briefly, 1.0 mg (0.58 μmol) of peptide was dissolved in 100 μL of DMF and mixed with 100 μL of a 58 mM solution of succinic anhydride in DMF (5.8 μmol, 10 equiv.). Then, 5 μL of a 0.1 M solution of DIPEA in DMF was added and the reaction was mixed for 6 h at room temperature. Modified peptide was diluted with PBS buffer (2 mL) and

purified from excess reagents using a nickel(II) nitrilotriacetic acid (Ni-NTA) agarose cartridge, and desalted using Amberchrom CG300M resin. The purified peptide was dried *in vacuo*.

The succinic acid-modified peptide was dissolved in 200 μL of DMF and mixed with 45 μL of a 20 mM solution of NHS (0.9 μmol) in DMF, followed by the addition of 32 μL of a 20 mM solution of DIC (0.64 μmol) in DMF. The reaction was mixed for 4 h at room temperature, then 20 μL of 50 mM solution of EZ-Link-PEG_3-biotin (1.0 μmol) in DMF was added and the reaction left to mix overnight at room temperature. Modified peptide was diluted with PBS buffer (2 mL), purified and desalted as described above, then dried *in vacuo* and stored at –20 °C until needed.

1.4 Preparation of Paper Test Strips

1.4.1 Dithiol-Modification of Cellulose

Cellulose paper was modified with bidentate thiol ligands according to Scheme 1, where the derivative of lipoic acid was synthesized as shown in Scheme 2. Chromatography paper (1.2 g, 5 circular sheets, 125 mm dia., Whatman, grade 4) were oxidized in 50 mL of 100 mM $NaIO_4$ in the dark for 1 h with mixing. Each paper sheet was washed three times with Nanopure water (Thermo Scientific, Waltham, MA, USA), twice with methanol, twice with dichloromethane (DCM) and dried *in vacuo*. Aldehyde-functionalized paper was immersed in 100 mL of dichloromethane (DCM) containing *ca.* 1 mmol of *N*-(2-aminoethyl)-5-(1,2-dithiolan-3-yl)pentanamide (see Scheme 2, as reported previously) for 12–16 h.

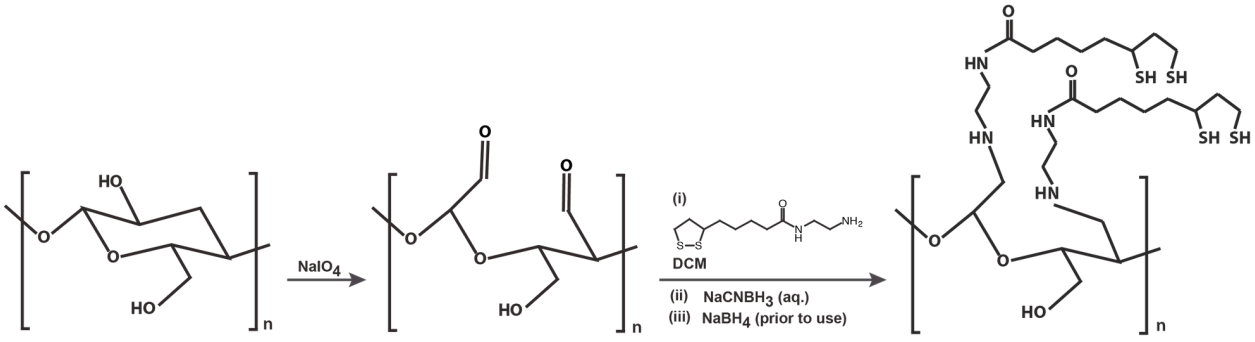

Scheme S1.

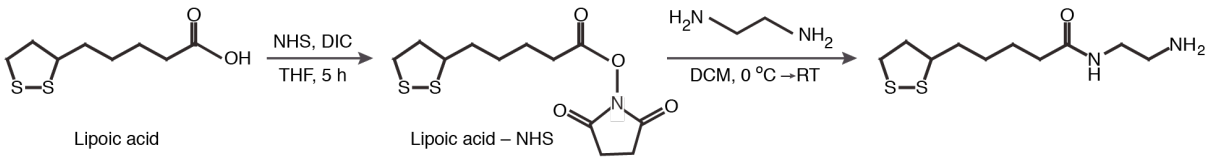

Scheme S2.

Functionalized paper sheets were rinsed three times with DCM, briefly air-dried, and immediately immersed in an aqueous solution of sodium cyanoborohydride (50 mM) for 1 h to reduce the imine bonds to secondary amines. Paper sheets were then rinsed thrice with Nanopure water, once with methanol, once with DCM, dried under vacuum, and stored in the freezer.

1.4.2 Sizing and Chemical Reduction

Paper sheets modified with the lipoic acid derivative, *N*-(2-aminoethyl)-5-(1,2-dithiolan-3-yl)pentanamide, were cut into rectangles (2 × 6 mm) or "test strips" using a paper punch (Recollections^{TM}, Michaels Stores, Inc., Irving, TX, USA). The paper test strips were added to solution of 50 mM sodium borohydride for 1–2 h to reduce disulfide groups to dithiols. The tests strips were then washed three times with water and once with ammonium acetate buffer (100 mM, pH 4.5). Excess buffer was removed by gently sandwiching paper substrates between dry sheets of lint-free tissues (Kimwipes, Kimberly Clark) three times and further air-drying for 5 min. Prolonged exposure to air (>20 min) prior to spotting QD solution was noted to produce less uniform QD immobilization, presumably due to reoxidation of the dithiols to disulfides.

1.4.3 Immobilization of QD-Peptide Conjugates

QD-peptide conjugates were prepared for sample and reference spots by mixing QD630 with the desired peptide at the desired concentration and ratio, as summarized in Table S2. All conjugates were prepared in borate buffer (50 mM, pH 9.2). The QD630–Pep(Biotin) and QD630–Pep conjugates were prepared in advance and stored at room temperature for up to one week. The QD630–Sub(A647) were prepared prior to use. In a typical experiment, solutions of QD630 and Sub(A647) were thoroughly mixed, incubated in the dark for 3–5 min. Next, 0.5 μL of this conjugate solution spotted directly on one end of the paper test strip placed in humid chamber, and the opposite end of paper test strip was then spotted with 0.5 μL of the reference conjugate, as illustrated in Figure S1. Test strips for thrombin assays were incubated inside the humid

chamber for 5–10 min, rinsed with borate buffer (5 mM, pH 9.2), dried on lint-free tissues and enclosed within the sample cells of a PDMS/glass chip. Test strips for competitive-binding SAv assays were washed with borate buffer (50 mM, pH 8.5, 50 mM NaCl), rinsed with 0.1% bovine serum albumin (BSA) in borate buffer, and finally rinsed once with borate buffer (5 mM, pH 8.5). The finished test strips were dried on lint-free tissues and enclosed within the sample cells of a PDMS/glass chip.

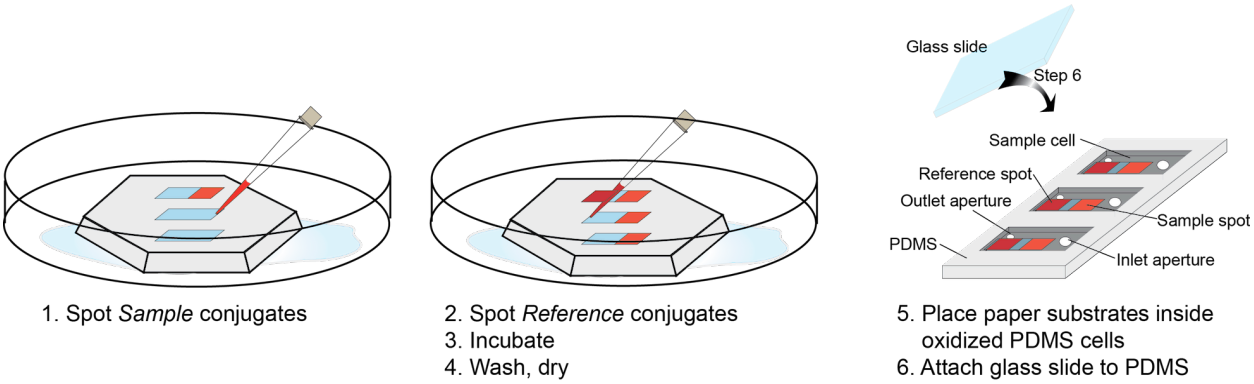

Figure S1. Preparation of paper substrates with immobilized QD-peptide conjugates and assembly of glass/PDMS chip containing paper substrate within sample cell.

Table S2. Spotted solutions of QD–peptide conjugates

Assay	Sample Spot	Reference Spot
Thrombin activity assay	Sub(A647)[a] QD:peptide Ratio 1:10 [QD630] = 4 μM [Sub(A647)] = 40 μM Volume spotted: 0.5 μL	Pep[a] QD:peptide Ratio 1:20 [QD630] = 1 μM [Pep] = 20 μM Volume spotted: 0.5 μL
Competitive-binding SAv assay	Pep(Biotin)[a] QD:peptide Ratio 1:20 [QD630] = 2 μM [Pep(Biotin)] = 40 μM Volume spotted: 0.5 μL	Pep[a] QD:peptide Ratio 1:20 [QD630] = 1 μM [Pep] = 20 μM Volume spotted: 0.5 μL

[a] Refer to Table S1 for the amino acid sequences of the peptides.

1.5 Fabrication of PDMS/Glass Chip

A positive-relief template for the sample cells and a holder for this template were fabricated from brass in-house (post-manufacture polishing is recommended). The template was the size of a standard glass microscope slide (~75 mm × 25 mm) and patterned 18 sample cells, each of which had dimensions of 4 mm × 9 mm × 250 μm ($l \times w \times h$). A schematic of the template is shown in Figure S2. PDMS chips were prepared from an elastomer kit by mixing elastomer base and curing agent in 10:1 w/w ratio. The mixture was degassed under vacuum for 40 min and *ca.* 3.0 g was poured over the template in its holder. PDMS was cured in the oven at 120 °C for 10 min, cooled, cut and peeled from the template. Cured PDMS was rinsed thoroughly with water and ethanol, then dried. Apertures were made at opposite ends of each sample cell with a 2 mm diameter punch (inlet for sample addition) and 1 mm diameter punch (outlet for air). The PDMS chip was placed upside down (recessed cells facing up) and air plasma oxidized for 60 s at 10.5 W. Finished test strips were then placed within the sample cells and a pre-cleaned (plasma treated) glass slide was pressed against the PDMS to form PDMS/glass chip. A photograph of a chip is shown in Figure 1 of the main manuscript.

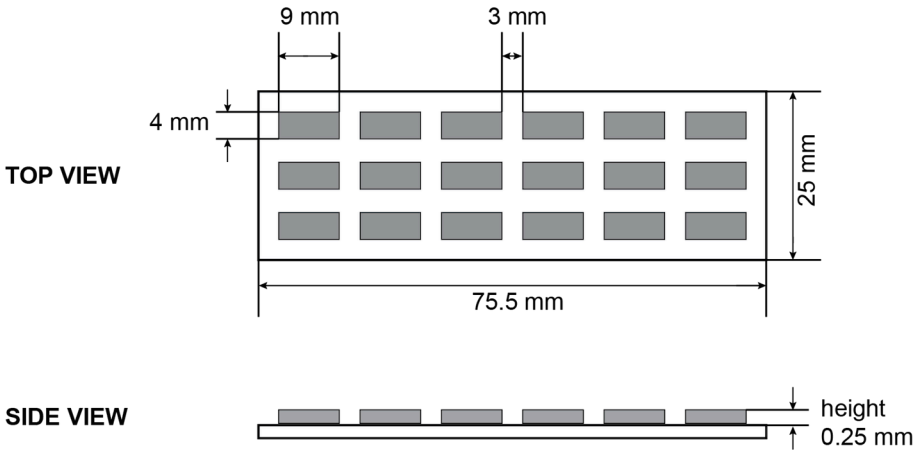

Figure S2. Drawing of a positive-relief template used to mould PDMS to form 18 sample cells on a microscope slide-sized chip.

1.6 Assay Procedures

1.6.1 Thrombin Assays

Human thrombin solutions were prepared in borate buffer (50 mM, pH 8.5), serum, 50% blood (prepared with borate buffer, pH 8.5), or whole blood. Thrombin stock solutions supplied by the vendor typically had activities in the range (22000–26000 NIH units mL^{-1}), so that even for the highest thrombin activities tested (*i.e.* 484 NIH units mL^{-1}), the content of the serum or whole blood in the sample was >96%. Protease activity was monitored by adding 12 μL of enzyme solution (7.6–480 NIH units mL^{-1}, or 63 nM–4 μM for a particular lot of enzyme) to the sample well containing paper substrates. An image (smartphone or USB-CMOS camera) was acquired prior to sample addition (noted as *dry sample*) and then after sample addition at 30 sec intervals for 30 min.

1.6.2 Competitive-Binding Streptavidin Assay

Six solutions were prepared in borate buffer (50 mM, pH 8.5, 50 mM NaCl) with 2.0 μM SAv-A647 and SAv at a concentration of 0, 0.4, 1.0, 2.0, 10, or 20 μM. These solutions (12 μL) were added to the sample wells containing paper tests strips. An image (smartphone) was acquired prior to sample addition (noted as *dry sample*) and then after sample addition at 30 sec intervals for 30 min. For SAv detection in 50% blood, a 15 μL volume samples containing SAv-A647 and SAv were prepared as described above and mixed with 15 μL volume of whole blood. The final concentrations were 1.0 μM SAv-A647 and 0, 0.2, 0.5, 1.0, 5.0 or 10 μM SAv.

1.7 Instrumentation and Data Acquisition

1.7.1 Characterization of LEDs

Several LEDs, listed in Tables S3, with emission maxima over the range 385–605 nm were evaluated as potential excitation sources. The LEDs were controlled and powered using LabVIEW software and a USB-6008 data acquisition (DAQ) module (National Instruments, Austin, TX, USA). LED emission spectra were obtained using a Green-Wave spectrometer (StellarNet, Tampa, FL, USA) coupled with an optical fiber (200 μm diameter; M25L01, Thorlabs, Newton NJ, USA). A neutral density filter (OD 3.0, Thorlabs) was used to reduce the LED intensity for acquisition of spectra. LED crosstalk was determined by collecting LED spectra using a longpass filter with a cutoff wavelength of 600 nm (FEL600, Thorlabs). A schematic of the setups used for acquisition of LED spectra is shown in Figure S3A. LED power

was measured with handheld laser power meter (Vega, Ophir-Spiricon LLC, North Logan, UT, USA).

Table S3. LEDs used for optimization experiments.

LED	Manufacturer / Supplier	Product number
1	Visual Communications Company, LLC	VAOL-5EUV8T4
2	Visual Communications Company, LLC	VAOL-5EUV0T4
3	Lee's Electronics	M506WCP
4	Lumex	LX509FT3U5BD
5	LEDtronics	LDF200-2PB-22
6	Lumex	LX9053UEGC
7	Everlight Electronics Co. Ltd.	EL-333-2UBGC/S400-A4
8	Fairchild Semiconductor Corp.	MV8G03
9	Kingbright	WP7143ZGC/G
10	Visual Communications Company, LLC	VAOL-5GDE4
11	Visual Communications Company, LLC	VAOL-5GCE4
12	Visual Communications Company, LLC	VAOL-5GSBY4

1.7.2 Absorbance, Transmittance and Fluorescence Measurements

Solution-phase PL spectra and absorbance spectra were acquired with either an Infinite M1000 fluorescence plate reader (Tecan US, Inc., Morrisville, NC, USA) or, when using LED excitation, the Green-Wave spectrometer. A schematic of the latter setup is shown in Figure S3B. PL emission and absorption spectra of immobilized QDs and QD-conjugates (see Figures 3–4 and Figure S13A) were obtained with an Infinite M1000 Pro by placing paper substrates between the windows of a NanoQuant plate (Tecan Ltd.).

PL images of paper samples were acquired using either (i) an iPhone 5S (Apple, Cupertino, CA, USA), or (ii) USB-CMOS monochrome camera (DCC1545; Thorlabs, Newton NJ, USA). For imaging experiments with PDMS/glass chip, two arrays of LEDs (VAOL-5GSBY4, 470 nm) connected in parallel (3.0–4.0 V applied, Table S4, S5) were used to illuminate the chip. A bandpass filter (624/40, center wavelength/bandwidth; Chroma, Bellows Falls, VT, USA) was used to isolate emission from QD630, and another bandpass filter (650/40, #FB650-40, Thorlabs) was used to isolate emission from QD650. A photograph of this setup is shown in

Figure 1 (main text) and a schematic is shown in Figure S3C. Image acquisition with the iPhone 5S was done using the Lapse It Pro application (Interactive Universe developer). Image acquisition with the USB-CMOS camera was done using micro-Manager software.[2] All image analysis was done using ImageJ software and the Time Series Analyzer 2.0 plug-in (National Institutes of Health, Bethesda, MD, USA).

The transmittance of LED light through paper substrates was measured on an inverted Olympus IX83 microscope (Olympus Canada Inc., ON, Canada) equipped with a sCMOS digital camera (ORCA-Flash 4.0, Hamamatsu) using a UV-transparent 96-well plate (Corning 3679). An increasing number of hydrated paper substrates (3 mm dia.) were placed in a well and an LED470 positioned for trans-illumination.

The effect of blood path length on the transmittance of light through blood was measured by pipetting a drop of blood between two glass slides separated by a defined distance using spacers (wetted cover slips with ~150 μm thickness). The bottom slide supported a test strip with immobilized QDs, held in place with tape. The path length was calculated from images acquired with 4× magnification lens. The length scale calibration was done using a calibration slide (Motic Instruments Inc., Richmond, BC, Canada). For measurement of QD630 PL (LED470 excitation) as a function of path length, images were acquired with a smartphone (iPhone 5S) or USB-CMOS monochrome camera and the intensities analyzed in ImageJ.

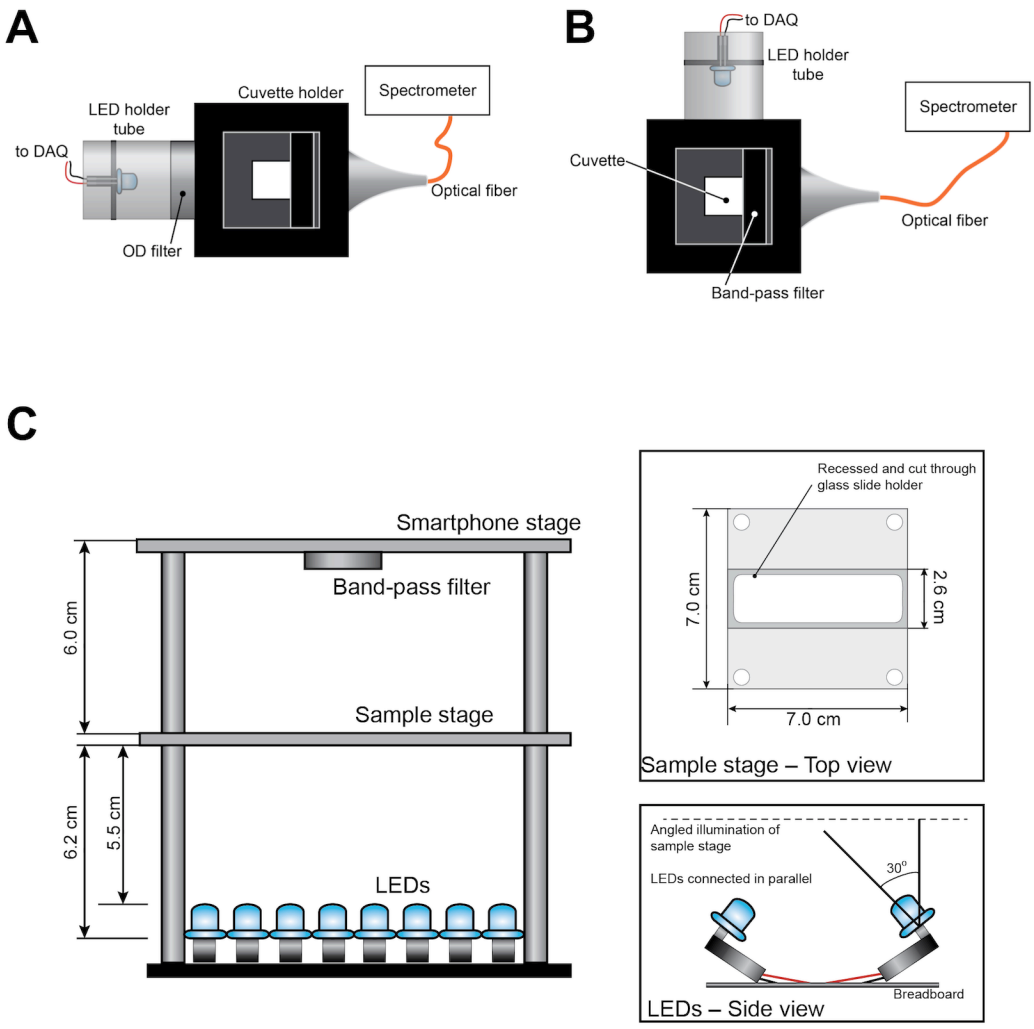

Figure S3. Schematics of the instrumental setups used for (A) acquisition of LED spectra, (B) solution-phase QD PL with LED excitation, and (C) color digital PL images with a smartphone. For the smartphone imaging, the pulsed LED source was powered from the USB connected DAQ module. Schematics are not to scale. A bandpass filter was used to isolate QD PL and reject reflected LED light and FRET-sensitized emission from dye-acceptor.

1.7.3 Sample Matrix-Dependent Image Acquisition Parameters

Table S4 and S5 summarize optimized parameters, including LED voltages and camera exposure times, used for QD PL imaging with either (i) an Apple iPhone 5S and the Lapse it Pro app, or (ii) a Thorlabs USB-CMOS monochrome camera and micro-Manager software.

Table S4. Acquisition parameters for iPhone and Lapse It Pro application.

Media	LED voltage (V)	Exposure	ISO	White Balance	Resolution
Buffer	3.0	1/60	544	0%	1080p
Serum	3.5	1/60	544	0%	1080p
50% blood	3.7	1/30	544	0%	1080p
Whole blood	4.0	1/20–1/15	544	0%	1080p

Table S5. Acquisition parameters for Thorlab CMOS camera and micro-Manager software.

Media	LED voltage (V)	Exposure	Gain
Buffer	3.5	10 ms	50
Serum	3.7	20 ms	50
50% blood	4.0	75 ms	50
Whole blood	4.0	100 ms	50

1.8 Data Analysis

1.8.1 FRET Parameters

The QD630-A647 and QD650-A680 FRET pairs were characterized using the Förster formalism. The Förster distance, $R_\circ$ (units of cm), was calculated using Eqn. S1,

$$R_\circ^6 = 8.79 \times 10^{-28}\,\text{mol} \times (n^{-4}\kappa^2\Phi_D J) \tag{S1}$$

where n = 1.335 is the refractive index of the surrounding medium, $\kappa^2 = 2/3$ (assumed) is the orientation factor, Φ_D is the quantum yield of the donor, and J is the spectral overlap. The spectral overlap was calculated according to Eqn. S2,

$$J = \frac{\int F_D(\lambda)\varepsilon_A(\lambda)\lambda^4\, d\lambda}{\int F_D(\lambda)\, d\lambda} \tag{S2}$$

where F_D is the fluorescence intensity of the donor, and ε_A is the molar absorption coefficient of the acceptor as a function of wavelength, λ. Rhodamine B in acidic ethanol ($\Phi = 0.49$)[3] was used as a standard for quantum yield measurements. The absorbance and fluorescence intensities of a

series of concentrations of QD630 and QD650 were measured with the plate reader and the slopes of plots of PL *versus* absorbance were used to determine the QD quantum yields.

$$\frac{\int PL_{QD}(\lambda_{em})d\lambda}{\int PL_{std}(\lambda_{em})d\lambda} = \frac{A_{QD}(\lambda_{exc})}{A_{std}(\lambda_{exc})}\left(\frac{\Phi_{QD}}{\Phi_{std}}\right)\left(\frac{\eta_{std}^2}{\eta_{QD}^2}\right) \tag{S3}$$

The FRET efficiency, E, was calculated from the PL measurements using Eqn. S4, where the terms F_D and F_{DA} are the fluorescence intensity of the QD donors (D) in the absence and presence of A647 or A680 acceptor (A), respectively.

$$E = 1 - \frac{F_{DA}}{F_D} \tag{S4}$$

1.8.2 Image and Data Analysis

Digital color images acquired with the iPhone 5S were split into corresponding R-G-B channels, and the average spot intensity, I, in the red channel was used for analysis. Digital images acquired with the monochrome USB-CMOS camera were used directly to calculate the average spot intensity, I. At each time point, t, a ratio between the sample and reference spot, $R(t)$, was calculated according to Eqn. S5, where the subscript S indicates the intensity of the sample spot, the subscript *Ref* indicates the intensity of the reference spot, and the notation *dry* refers to the images acquired prior to sample addition. For 50% blood and whole blood samples, dry images were acquired with the buffer acquisition parameters (see Table S4-S5).

$$R(t) = \frac{I_S(t)/I_S(\text{dry})}{I_{\text{Ref}}(t)/I_{\text{Ref}}(\text{dry})} \tag{S5}$$

Thrombin assays were done with a control sample that had no added thrombin, $[E] = 0$. As shown in Eqn. S6, each of the values of $R(t)$ (Eqn. S5) for a given enzyme activity, $[E]$, were normalized to an initial value of unity by dividing by the ratio at $t = 0$ (*i.e.*, immediately after sample addition), and all subsequent time points were then scaled to the control sample.

$$R_N(t) = \frac{R_{[E]}(t)/R_{[E]}(0)}{R_{[E]=0}(t)/R_{[E]=0}(0)} \tag{S6}$$

Normalized progress curves were fit with an exponential function in ProFit software (QuantumSoft, Bühlstr, Switzerland) using Eqn. S7. Average rates were calculated according to Eqn. S8.

$$R_{N,t} = A_2\left(2-\left(A_1\exp(-k_1x)\right)-\left(\left(2-A_1\right)\exp\left(-k_2x\right)\right)+C \tag{S7}$$

$$k_{av} = \frac{A_1k_1+\left(2-A_1\right)k_2}{A_1+\left(2-A_1\right)} \tag{S8}$$

2. Additional Results and Discussion

2.1 QD630 *versus* QD650 for Blood Measurements

As shown in Figure S4, blood exhibits strong absorption across most of the UV-visible spectrum with minimal absorption in the red region (*ca.* 600–700 nm). Two QDs with emission centered at 630 nm and 650 nm were evaluated. The absorption and emission spectra of QD630 and QD650 are shown in Figure S4. The broad and strong absorption of QDs from < 400 nm to *ca.* 600 nm permitted selection of an optimum excitation wavelength that was a compromise between minimizing the attenuation of excitation light by blood and the wavelength-dependent molar absorption coefficients of the QDs. Bandpass (BP) filters were used for imaging QDs with a smartphone (iPhone 5S) and USB-CMOS monochrome camera (elimination of reflected and scattered excitation light). The transmission of the BP624/40 and BP650/40 filters used with QD630 and QD650, respectively, are shown in Figure S4.

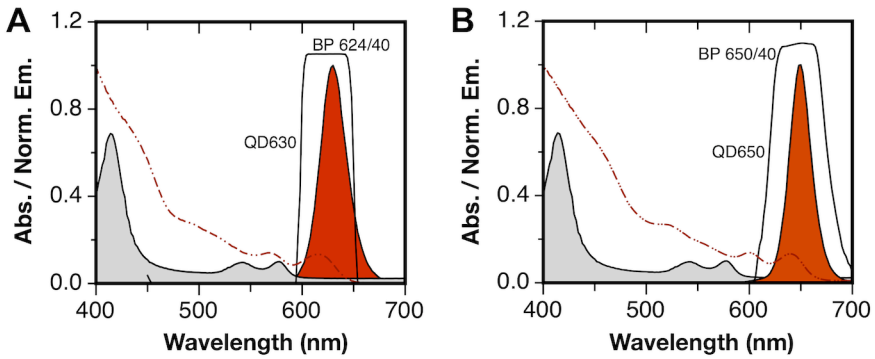

Figure S4. Normalized absorption and PL spectra for the (A) QD630 **(A)** and **(B)** QD650. The transmission spectra of the bandpass filters are shown as solid black lines and the absorption spectrum of a 0.05% blood sample (path length = 1 cm) is shown as a shaded grey region.

2.2 QD630-A647 and QD650-A680 FRET Pairs

The absorption and PL spectra for QD630 and A647, and QD650 and A680, are shown in Figure S5. Table S6 summarizes the FRET systems. From fitting the FRET efficiency curves shown in Figure S6 (corrected for the Poisson distribution of acceptors),[4] the donor-acceptor separation distances for QD630-A647 and QD650-A680 FRET pairs were estimated to be *ca.* 10.9 and 12.4 nm, respectively. These distances include both the radii of the QDs (see Table S6) and the extension of the peptide. The maximum peptide extension is expected to be 8.7 nm (using an estimate of 23 amino acids and a length of 0.38 nm per residue, with the assumption that the six histidine residues are bound to the QD surface and do not contribute to extension of the peptide).

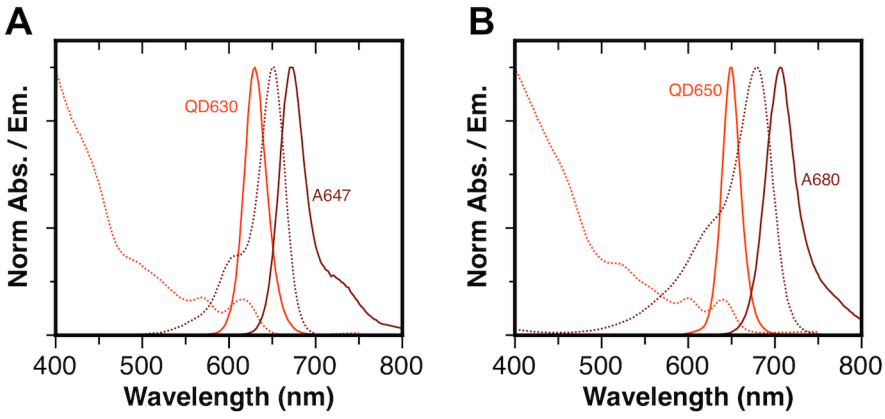

Figure S5. Normalized absorption and emission spectra for **(A)** the QD630-A647 FRET pair and **(B)** the QD650-A680 FRET pair. Absorption spectra are shown as dotted lines and emission spectra are shown as solid lines.

Table S6. Photophysical parameters of QD630-A647 and QD650-A680 FRET pairs

QD	$\lambda_{max,em}$ [a]	FWHM [b]	Dye	$\varepsilon_{A,max}$ [c]	Φ_{QD} [d]	$\varnothing_{QD}$ (nm) [f]	J ($cm^6\ mol^{-1}$) [g]	R_o (nm)	r (nm)
QD630	630	29	A647	250 000	0.77	5.2	2.3×10^{-9}	7.8	10.9
QD650	652	25	A680	175 000	0.25	7.2	2.0×10^{-9}	6.2	12.4

[a] Maximum emission wavelength of QD; [b] full-width-at-half-maximum; [c] molar absorption coefficient of the dye at its absorption maximum; [d] quantum yield of the QD; [f] Approximate diameter of the QD nanocrystal; [g] spectral overlap integral.

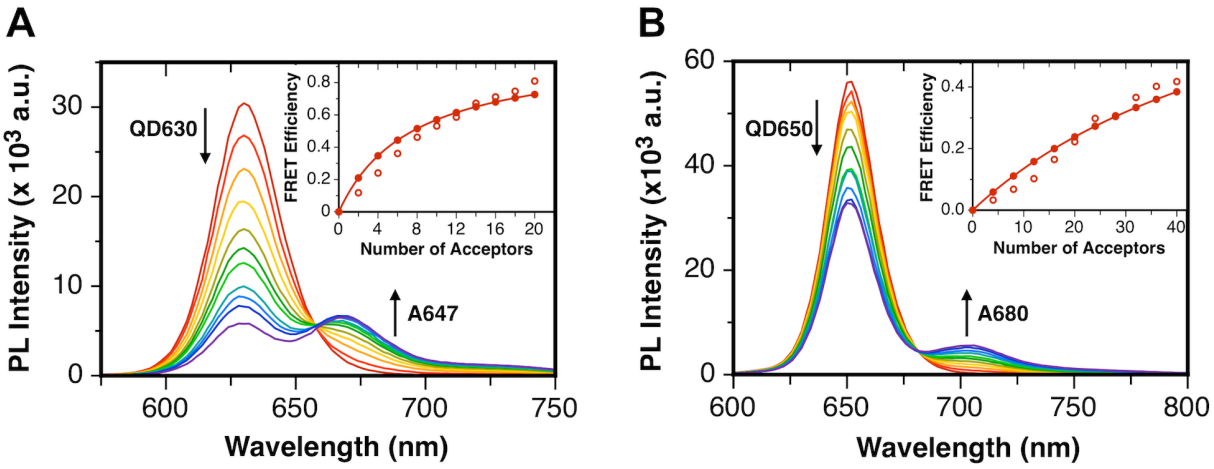

Figure S6. Solution-phase FRET: **(A)** PL emission spectra showing assembly of an increasing number Sub(A647) per QD630; **(B)** PL emission spectra showing assembly of an increasing number of Sub(A680) per QD650. The insets in panel (A) and (B) show the FRET efficiencies calculated from quenching of QD PL as a function of the number of acceptors per QD (open circles, raw data; closed circles, Poisson corrected data).

2.3 Selection of an LED Excitation Source

Twelve models of low-cost T-1 3/4 (5 mm) LED light sources (Table S7) were characterized as a potential excitation source for QD630 and QD650. A few representative emission profiles of these LEDs are shown in Figure S7. Comparison between these LEDs and selection of the optimal LED for assays in whole blood was based on several parameters: (i) brightness, (ii) the efficiency of QD excitation, (iii) the magnitude of crosstalk with QD detection channel, and (iv) overlap with blood absorption spectrum.

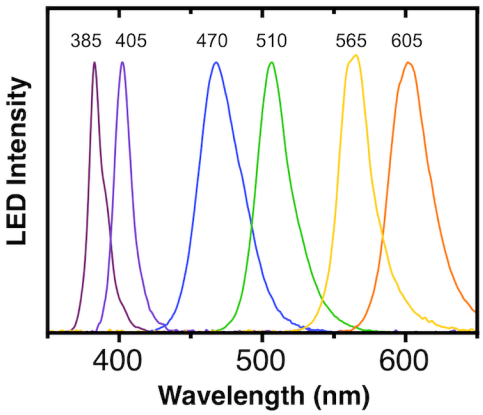

Figure S7. Emission spectra of selected LEDs that were evaluated as excitation sources for QD-based assays in serum and whole blood. The emission wavelengths for all LEDs tested are listed in Table S7-A.

LEDs were turned on with the applied voltage indicated by the manufacturer (Table S7-B). The LED spectra were collected with a portable spectrometer and the integrated emission intensities were calculated (Table S7-B) to identify the brightest LEDs (Table S7, LED No. 5, 7, 8, and 10). These results largely correlated with those obtained by measuring the LED output with an optical power meter (Table S7-E).

Next, the ability of LEDs to excite QD630 and QD650 PL was evaluated. Aqueous samples of QDs were illuminated with an LED (setup in Figure S3B) and QD PL spectra acquired with a portable spectrometer. The relative QD PL intensity between LED excitation sources was calculated according to Eq. S9. The results are summarized in (Table S7-G, J).

$$PL_{QD} = \left(\int_{550}^{750} I_{QD} \Big/ \left[\int_{550}^{750} I_{QD} \right]_{MAX} \right) \times 100\% \qquad \text{(S9)}$$

The magnitude of integrated QD PL intensity was dependent on the brightness of an LED, the size of QD molar absorption coefficient over the wavelength range of LED emission, and the quantum yield of the QD. The QD630 and QD650 molar absorption coefficients at the peak LED emission wavelengths are indicated (Table S7-F, I). The strongest QD PL was observed with a blue LED470 (Table S7, LED No. 5), followed by a green LED 525 (LED No. 10), and a UV LED385 (LED No. 1).

Another important factor in LED selection is the extent of crosstalk with the QD detection channel, as scattered excitation light was unavoidable in our assays and optical filters are imperfect. The relative LED crosstalk, X_{LED}, in the putative red channel for smartphone imaging (600–650 nm) was calculated according to Eq. S10 from spectrometer measurements (Table S7-C). As expected LEDs with emission in the green-yellow region of the spectrum had the greatest crosstalk from their emission tails.

$$X_{LED} = \left(\int_{600}^{650} I_{LED} \Big/ \int_{350}^{700} I_{LED} \right) \times 100\% \tag{S10}$$

Furthermore, to evaluate LED crosstalk under conditions similar to the assay, we acquired LED spectra with a longpass filter (600 nm cutoff) and calculated the LED crosstalk relative to the QD PL intensity measured upon excitation with the LED of interest. The relative crosstalk was calculated according to Eqns. 11–12 (Table S7-H,K).

$$X_{LED/QD630} = \left(\int_{604}^{644} I_{LED} \Big/ \int_{604}^{644} I_{QD630} \right) \times 100\% \tag{S11}$$

$$X_{LED/QD650} = \left(\int_{630}^{670} I_{LED} \Big/ \int_{630}^{670} I_{QD650} \right) \times 100\% \tag{S12}$$

All LEDs had negligible crosstalk in the QD650 channel (650/50 filter), whereas the largest crosstalk in QD630 channel (625/50 filter) was noted with yellow-emitting LEDs. This result was due to a combination of an inefficient excitation of the QD (lower intensity LED, smaller absorption coefficient at those wavelengths) and an LED emission profile that tailed into the red region of the spectrum. Less than 1% crosstalk was calculated for the UV and blue-emitting LEDs. Although some of the crosstalk values may appear small, it is important to note that LED emission is many times bright than QD PL.

Given the foregoing evaluation of candidate LEDs, and the efficiency of QD excitation and minimization of crosstalk, five LEDs emerged as leading candidates: a blue LED (No. 5), green LEDs (No. 7,8 and 10), and a UV LED (No. 1). These five LEDs were further compared by

exciting paper-immobilized QDs soaked in blood. No QD PL was observed upon excitation with UV LED, primarily due to the strong absorption and scattering of these wavelengths by blood. Between the green LEDs and blue LED, excitation of immobilized QDs in a blood matrix with a blue LED provided a more than 8-fold better signal-to-background ratio (Table S7, LED No. 5). This result was due to both the spectral characteristics of the LED and its intensity level. Therefore, LED470 (No. 5) was used as the excitation source for all assays.

Table S7. Characterization of LEDs as excitation sources for QD630 and QD650.

LED	(A) λ_{max}	(B) I_{LED} (%)	(C) X_{LED} (%)	(D) V_{appl}	(E) Output	(F) ε_{QD630} ($\times 10^5$ cm^{-1} M^{-1})	(G) PL_{QD630} (%)	(H) $X_{LED/QD630}$ (%)	(I) ε_{QD650} ($\times 10^5$cm^{-1} M^{-1})	(J) PL_{QD650} (%)	(K) $X_{LED/QD650}$ (%)
1	385	1.1	0.24	3.6 V	1.44 mW	36.0	46.2	0.02	71.6	41.0	0.007
2	405	3.0	0.09	3.6 V	1.32 mW	28.2	19.7	0.04	62.4	19.7	0.014
3	470	7.8	0.04	3.6 V	1.23 mW	11.0	20.0	0.015	32.0	19.7	0.007
4	470	0.3	0.07	3.8 V	0.60 mW	11.0	2.0	0.006	32.0	2.1	0.006
5	470	72.0	0.01	4.0 V	3.80 mW	11.0	100.0	0.019	32.0	100.0	0.006
6	465	5.9	0.01	3.8 V	0.97 mW	12.6	17.4	0.013	36.0	18.3	0.005
7	500	40.9	0.09	4.0 V	2.90 mW	8.42	37.9	0.32	18.2	35.0	0.061
8	510	100.0	0.07	4.0 V	2.53 mW	7.87	29.1	0.74	17.6	27.3	0.13
9	525	41.5	0.39	4.0 V	1.86 mW	6.79	21.6	2.6	17.2	21.7	0.34
10	525	36.2	0.39	4.0 V	2.14 mW	6.79	65.0	0.56	17.2	63.7	0.065
11	565	2.6	0.73	2.4 V	0.66 mW	5.03	0.01	662	10.4	0.0	286
12	585	0.1	21.5	2.4 V	0.59 mW	3.84	0.03	285	7.85	0.1	22

(A) λ_{max} = wavelength of maximum emission; (B) I_{LED} = integrated intensity of LED relative to the LED with highest intensity; (C) X_{LED} = crosstalk of the LED in 600–650 nm spectral range (Eqn. S10); (D) V_{appl} = applied LED voltage ; (E) light output from the LED at the specified voltage; (F, I) ε_{QD} = molar absorption coefficient of the QD at the peak LED emission wavelength; (G, J) PL_{QD} = relative QD PL with LED excitation calculated (Eqn. S9); (H, K) $X_{LED/QD}$ = crosstalk of the LED relative to the QD PL (Eqns. S11-S12).

2.4 Path Length Through Blood and Paper Transmittance

The biggest determinant of the QD630 PL intensity measured from test strips was the optical path length through blood samples. To characterize the signal loss as a function of path length, the simple setup shown in Figure S8A was used (see Section 1.8.2 for details) and images of QD630 PL acquired with a smartphone (iPhone 5S) or USB-CMOS monochrome camera. The results are shown in Figure S8B. The maximum measureable intensity in blood was observed at the shortest path length we could produce, 250–300 μm, and this value was arbitrarily set to 100%. The QD630 intensity quickly decreased as the path length increased, to a degree that even millimeter path lengths were impractical. Consequently, a disposable chip was designed to provide a reproducibly short path length.

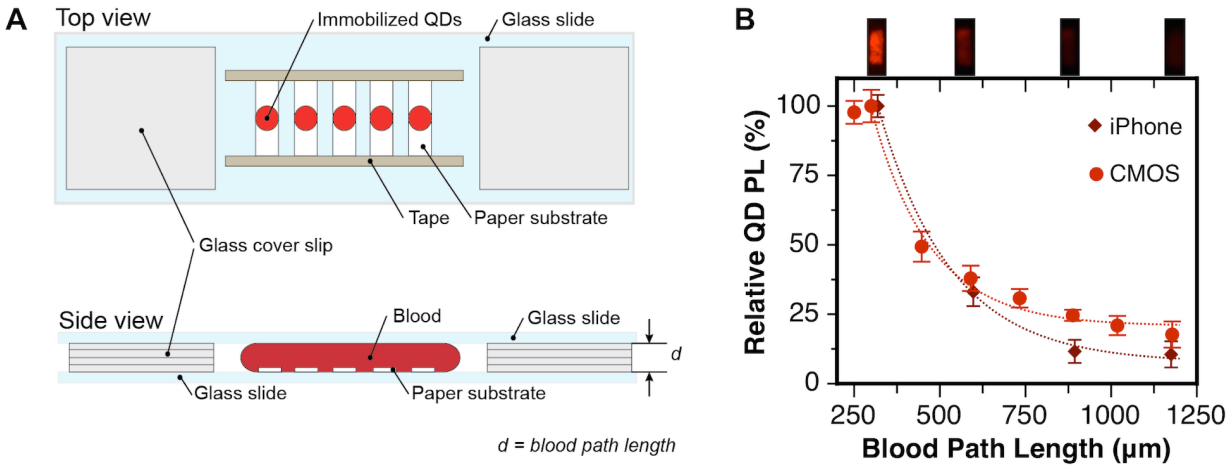

Figure S8. (A) Experimental design to determine effect of blood path length on measured PL intensity of immobilized QDs. The paper substrates were placed between two glass slides and distance separation was controlled by placing cover slips (n = 1–8) between them. (B) Effect of blood path length on attenuation of QD630 PL intensity from paper substrates measured with iPhone and CMOS monochrome camera.

Another factor that limited the brightness of QD630 PL was the intensity of excitation light that could be delivered. Trans-illumination of the spots of QD630 with LED470 light provided better signal-to-background ratios than epi-illumination. Although trans-illumination was more favorable than epi-illumination, the attenuation of excitation light by the paper test strip was nonetheless non-trivial. Only ~5% of the incident excitation was transmitted directly through a paper test strip, and an exponential decrease in transmission was observed with increasing paper thickness (*i.e.*, paper layers in our experiment). It is important to note that the values in Figure S9

represent transmitted intensities. Since QDs were immobilized throughout the thickness of the paper, QDs near the face of the paper closest to the LED experienced much greater excitation intensity than those on the opposite face. With epi-illumination, in the case that the test strip was at the bottom of a blood sample with a non-trivial path length, the excitation light was attenuated by the blood before reaching the near face of the paper test strip, resulting in lower average excitation intensity for the QDs than with trans-illumination. In addition, attenuation of excitation light by paper and blood in the trans-illumination configuration also minimized the amount of excitation light reaching the detection optics.

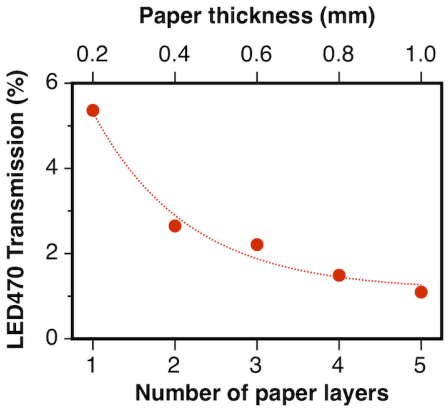

Figure S9. Effect of thickness of the paper on the intensity of LED470 light transmitted through chemically modified Whatman chromatography paper No. 4 soaked in buffer.

2.5 Representative Raw Data from Thrombin Assays with Smartphone Imaging

Figure S10 shows average spot intensities that were used to calculate the normalized progress curves shown in Figure 3 of the main text.

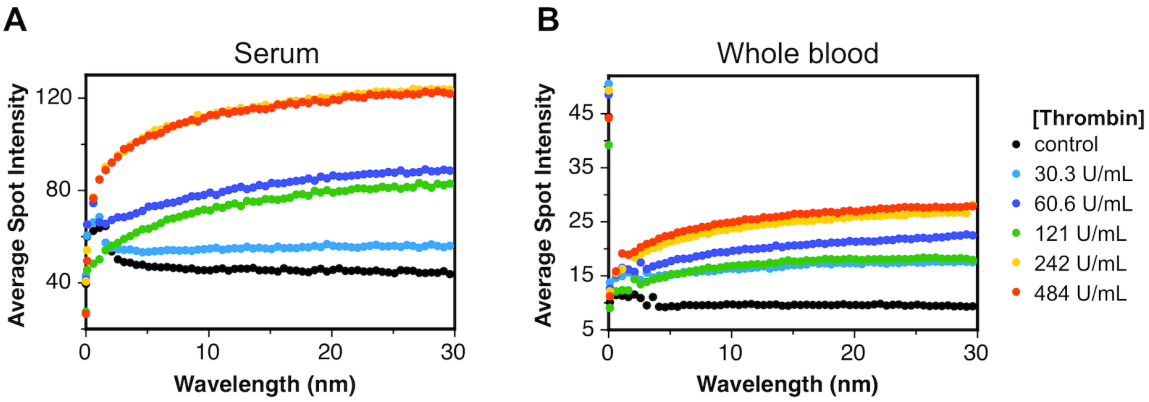

Figure S10. Raw data (as average spot intensity) measured from imaging sample spots as a function of time upon exposure to increasing activities of thrombin in (A) serum and (B) whole blood. Thrombin activity is measured in NIH units mL^{-1}.

2.6 Thrombin Assays with USB-CMOS Monochrome Camera Imaging

Thrombin activity-assays were possible with not only smartphone cameras, but also with other CMOS cameras. To this end, we also evaluated a USB-CMOS monochrome camera for readout of thrombin assays in buffer, serum, 50% blood, and whole blood. Figure S11 shows the progress curves obtained from digital images.

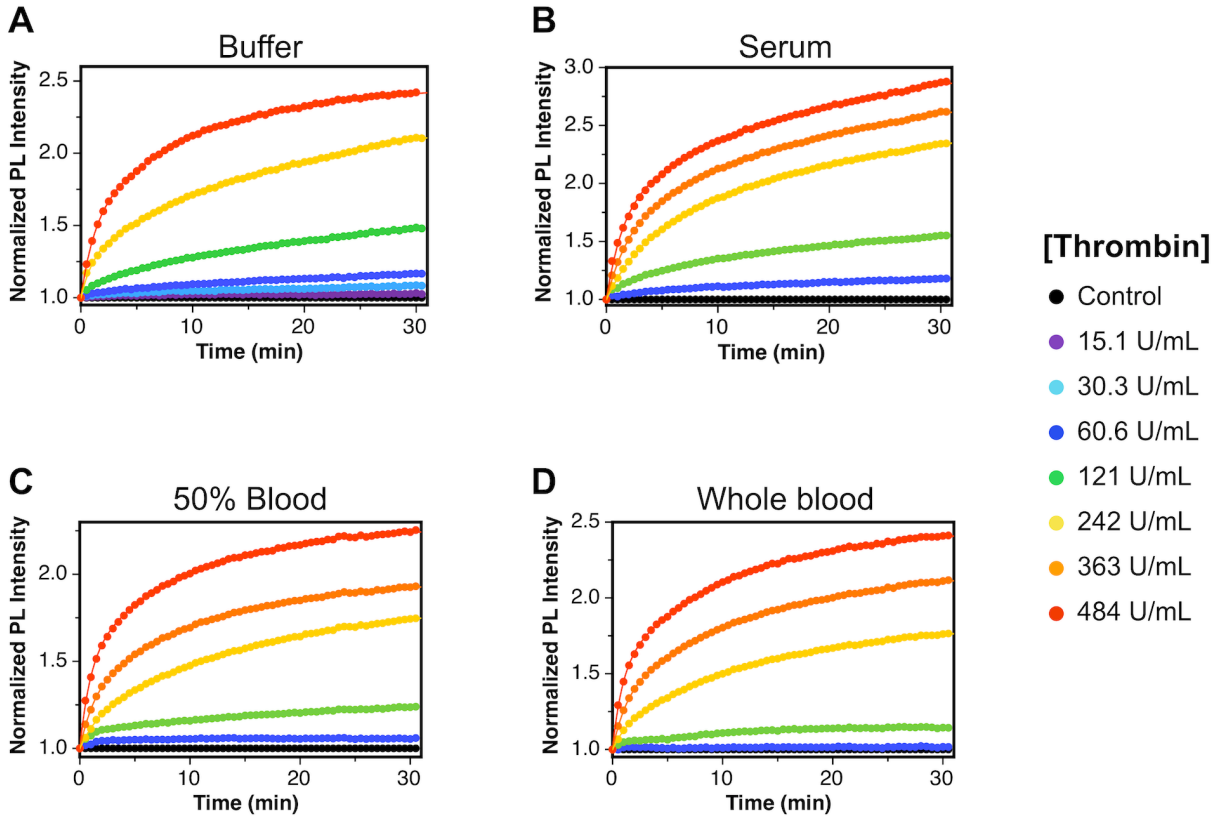

Figure S11. Progress curves for thrombin activity in **(A)** buffer, **(B)** serum, **(C)** 50% blood, and **(D)** whole blood from the images acquired with CMOS monochrome camera upon exposure paper substrates to increasing thrombin activity (measured as NIH units mL^{-1}).

2.7 Thrombin Blind Assays

To further test our assay format with whole blood samples, blind assays were done with spiked samples. Whole blood samples spiked with three activities of human thrombin were analyzed as five replicates in the sample chip. The resulting progress curves are shown in Figure S12. The average rate of change in QD630 PL intensity was calculated from this data (Eqn. S8) and used to estimate the amount of thrombin in the samples (see Table 2, main text) based on calibration data (Figure S11).

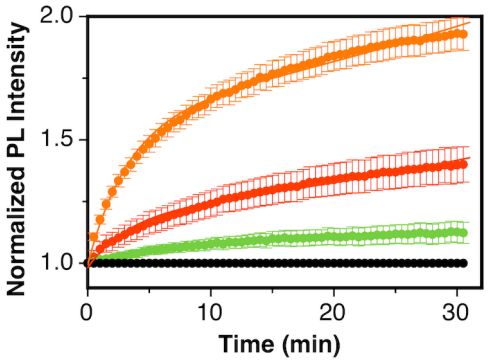

Figure S12. Progress curves for the detection of thrombin activity in blind samples. Error bars describe standard deviation (n = 5).

2.8 Competitive-Binding Streptavidin Assays

A general competitive-binding assay format was demonstrated in addition to the activity-based thrombin assay. In the competitive format, streptavidin (SAv) was used as a model analyte and FRET was modulated through a competition between native and A647-labeled SAv for biotin binding sites on QD630 immobilized on paper test strips. Figure S13A shows spectra of immobilized QD630-Pep(Biotin) assembled with increasing number of SAv per QD. Each Sav was labeled with *ca.* 5 A647 dyes and the FRET efficiency (estimated from QD630 PL quenching) was *ca.* 75%. Assay data is shown in Figure S13B-C for buffer and 50% blood. The quenching of QD PL decreased with increasing amounts of unlabeled streptavidin, which successfully competed for biotin-binding sites on the immobilized QD630, limiting the formation of QD630-A647 FRET pairs.

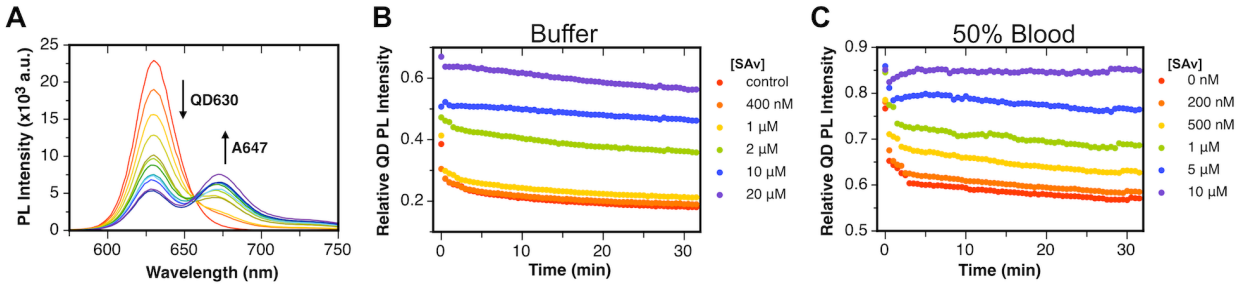

Figure S13. (A) PL emission spectra corresponding to the increasing number of SAv-A647 binding to immobilized QD630-Pep(biotin) conjugates. The number of SAv per QD were 0, 0.5, 1, 1.5, 2, 2.5, 3, 3.5, 4, 4.5, 5, and 6. The other panels show data from paper-based competitive SAv assays in **(B)** buffer and **(C)** 50% blood. The data is the relative QD PL intensity as a function of time upon exposure to different concentrations of SAv (analyte) and a fixed concentration of SAv-A647 (competitor). For assays in buffer, the concentration of SAv-A647 was 2.0 µM, whereas the concentration for assays in 50% blood was 1.0 µM.

3. References

1. W. R. Algar, J. B. Blanco-Canosa, R. L. Manthe, K. Susumu, M. H. Stewart, P. E. Dawson and I. L. Medintz, *Meth. Mol. Biol.*, 2013, **1025**, 47-73.
2. A. D. Edelstein, M. A. Tsuchida, N. Amodaj, H. Pinkard, R. D. Vale and N. Stuurman, *Journal of Biological Methods*, 2014, **1**, e10.
3. K. G. Casey and E. L. Quitevis, *J. Phys. Chem.*, 1988, **92**, 6590-6594.
4. T. Pons, I. L. Medintz, X. Wang, D. S. English and H. Matoussi, *J. Am. Chem. Soc.*, 2006, **128**, 15324-15331.